Table 1 Characteristics of 382 patients with hepatitis C treated with interferon therapy in this study

Age (years)	59.0 (18–81)
[a]Males/females	192/190
Observation period (years)	4.1 (0.1–8.4)
[a]IFN + RBV/PEG-IFN + RBV	69/313
HCV genotype 1/2/unclassified	229/57/96
HCV RNA (log IU/mL)	6.1 (2.3–7.3)
White blood cell count (/μL)	4950 (2050–9970)
Hemoglobin (g/dL)	14.0 (10.3–18.8)
Platelet (10^4/μL)	15.0 (5.3–36.4)
AST (IU/L)	56 (17–244)
ALT (IU/L)	67 (16–416)
Bilirubin (mg/dL)	0.8 (0.3–2.4)
AFP (ng/mL)	6.9 (1.6–478.3)

Qualitative variables ([a]) are shown in number, and quantitative variables expressed as median (range)

IFN interferon, *RBV* ribavirin, *PEG-IFN* pegylated interferon, *AST* aspartate aminotransferase, *ALT* alanine aminotransferase, *AFP* alpha-fetoprotein

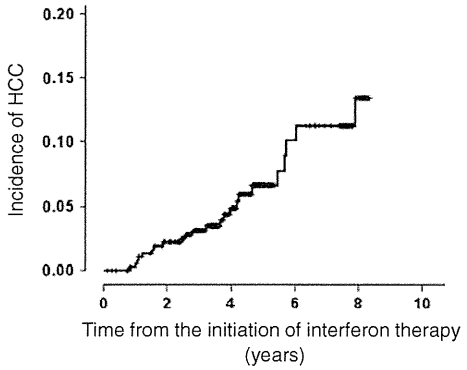

Fig. 2 Incidence of hepatocellular carcinoma (HCC) in 382 patients with hepatitis C who received interferon therapy, estimated using the Kaplan–Meier method

Table 2 Univariate analysis of predictive factors for incidence of hepatocellular carcinoma in all 382 and 197 non-SVR patients

Factors	All (n = 382)			Non-SVR (n = 197)		
	No.	Incidence of HCC (n = 23)		No.	Incidence of HCC (n = 22)	
		No. (%)	P value[a]		No. (%)	P value[a]
Age (years)						
<70	359	19 (5)	0.040	182	18 (10)	0.089
≥70	23	4 (17)		15	4 (27)	
Sex						
Female	190	8 (4)	0.125	111	8 (7)	0.022
Male	192	15 (8)		86	14 (16)	
HCV genotype						
1	229	12 (5)	0.452	137	12 (9)	0.796
Non-1	57	1 (2)		10	1 (10)	
Virological response						
SVR	185	1 (1)	<0.0001			
Non-SVR	197	22 (11)				
Biochemical response						
SBR	282	12 (4)	0.027	102	11 (11)	0.857
Non-SBR	86	11 (13)		81	11 (14)	
ALT before IFN therapy						
<40	79	2 (3)	0.274	39	2 (5)	0.319
≥40	301	21 (7)		158	20 (13)	
ALT integration value						
<40	238	6 (3)	0.001	79	5 (6)	0.153
≥40	142	17 (12)		118	17 (14)	
AFP before IFN therapy						
<10	230	7 (3)	0.005	102	7 (7)	0.124
≥10	116	14 (12)		75	13 (17)	
AFP integration value						
<10	258	8 (3)	<0.0001	115	8 (6)	0.019
≥10	63	12 (19)		53	11 (21)	
Platelet before IFN therapy						
<150,000	187	20 (11)	0.001	121	19 (16)	0.022
≥150,000	194	3 (2)		76	3 (4)	

[a] Log-rank test

SVR sustained virological response, *SBR* sustained biochemical response, *ALT* alanine aminotransferase, *IFN* interferon, *AFP* alpha-fetoprotein

Further, although patients with average AFP integration values ≥10 ng/mL also appeared to have an increased risk of HCC, the difference did not reach statistical significance in the multivariate analysis (P = 0.050) (Table 3).

Predictive factors for incidence of HCC in non-SVR patients

Because non-SVR was the only predictive factor across the entire study cohort, to clarify predictive factors for incidence of HCC within this group, the same variables were further analyzed in non-SVR patients alone. By univariate analysis, average AFP integration value ≥10 ng/mL (P = 0.019) and baseline platelet count <150,000 (P = 0.0022) (Table 2) were again identified as significant predictive factors for incidence of HCC. In addition, male gender was significantly associated with incidence of HCC in non-SVR patients (P = 0.022). Multivariate analysis, however, indicated that only two variables were independently associated with incidence of HCC in non-SVR patients: average AFP integration value ≥10 ng/mL (HR 4.039, 95% CI 1.570–10.392, P = 0.004), and male gender

Table 3 Multivariate analysis of the predictive factors for incidence of hepatocellular carcinoma in all 382 patients

Factors	Hazard ratio	95% CI	*P* value
Virological response			
SVR	1		
Non-SVR	8.413	1.068–66.300	0.043
AFP integration value			
<10	1		
≥10	2.580	0.999–6.659	0.050

SVR sustained virological response, *IFN* interferon, *AFP* alpha-fetoprotein

Table 4 Multivariate analysis of predictive factors for incidence of hepatocellular carcinoma in 197 non-SVR patients

Factors	Hazard ratio	95% CI	*P* value
AFP integration value			
<10	1		
≥10	4.039	1.570–10.392	0.004
Sex			
Female	1		
Male	3.636	1.383–9.563	0.009

AFP alpha-fetoprotein

(HR 3.636, 95% CI 1.383–9.563, $P = 0.009$) (Table 4). There was no significant difference in other variables including those identified as predictive factors in the entire study population (i.e., age, non-SBR, ALT integration value, AFP before interferon therapy) (Table 2).

AFP integration value as a predictive factor for HCC

Further analysis focused on the AFP integration value as this was the strongest predictive factor for incidence of HCC in non-SVR patients. Of the 382 patients, both baseline and AFP integration values were available for 321. These were divided into four groups: (1) AFP "low–low," (2) AFP "low–high," (3) AFP "high–low," and (4) AFP "high–high," for baseline AFP-average AFP integration values, respectively, where "high" is ≥10 ng/mL and "low" is <10 ng/mL. As shown in Fig. 3a, of the 321 patients, 211 (65.7%) showed baseline AFP levels <10 ng/mL. Of these 211, 207 (98%), were in the AFP low–low group, and only four in the AFP low–high groups. Baseline characteristics, including age, gender, serum HCV-RNA, aspartate aminotransferase (AST), ALT, bilirubin, white blood cell, hemoglobin, platelet, observation periods, and number of times of AFP measurement, were not different between AFP high–low group and high–high group. However, AFP-low group, which is a combination of the low–high and low–low groups, showed significantly lower AST level ($P < 0.00001$), lower ALT level ($P < 0.00001$), higher platelet count ($P < 0.00001$), shorter observation period ($P = 0.01448$), and fewer number of times of AFP examination ($P = 0.00035$), compared to both AFP high–high and AFP high–low group. Six patients (2.8%) with baseline AFP levels <10 ng/mL developed HCC in the follow-up period and none of these patients were among the four low–high group patients. Even in patients with high baseline AFP levels, incidence of HCC was only 3.9% among the AFP high–low group (2 of 51 patients). In contrast, 20.3% of patients in the AFP high–high group developed HCC during the follow-up period.

The incidence rate of HCC in three patient groups, "AFP-low" (a combination of the "low–high" and "low–low" groups),"high–low," and "high–high", was estimated using the Kaplan–Meier method and compared using log-rank tests (Fig. 3b). The rate of HCC incidence was significantly higher in the AFP high–high group compared to both the AFP high–low group and patients with low baseline AFP levels ($P = 0.009$ and 0.001, respectively). There was no significant difference between patients with low baseline AFP levels and the AFP high–low group. The 7-year incidence rate of HCC was 32.3% in the AFP high–high group, compared to only 6.6% in the AFP high–low group, and 8.1% in all patients with low pre-treatment levels.

Discussion

It is well recognized that the most effective strategy for the prevention of HCC development in patients with chronic hepatitis C is likely to be the complete elimination of the HCV infection accompanied by the resultant normalization of liver function [7, 12, 13, 15, 16, 19]. Indeed, we confirmed here that non-SVR is the most significant predictive factor for incidence of HCC in patients receiving interferon therapy for chronic hepatitis C. However, it should be noted that the risk of HCC, even in non-SVR patients, differs between individuals. In the current study, we identified AFP integration value and male gender as independent risk factors for incidence of HCC in non-SVR patients. The incidence of HCC was significantly reduced in individuals with average AFP integration values < 10 ng/mL after interferon therapy, which suggests that the decrease of AFP by interferon therapy lowers the risk of developing HCC. Indeed, even where patients had high baseline AFP levels, incidence of HCC was reduced when the AFP integration value decreased after interferon therapy. Thus, our current findings identify AFP integration value as a useful predictive marker of HCC development in non-SVR patients.

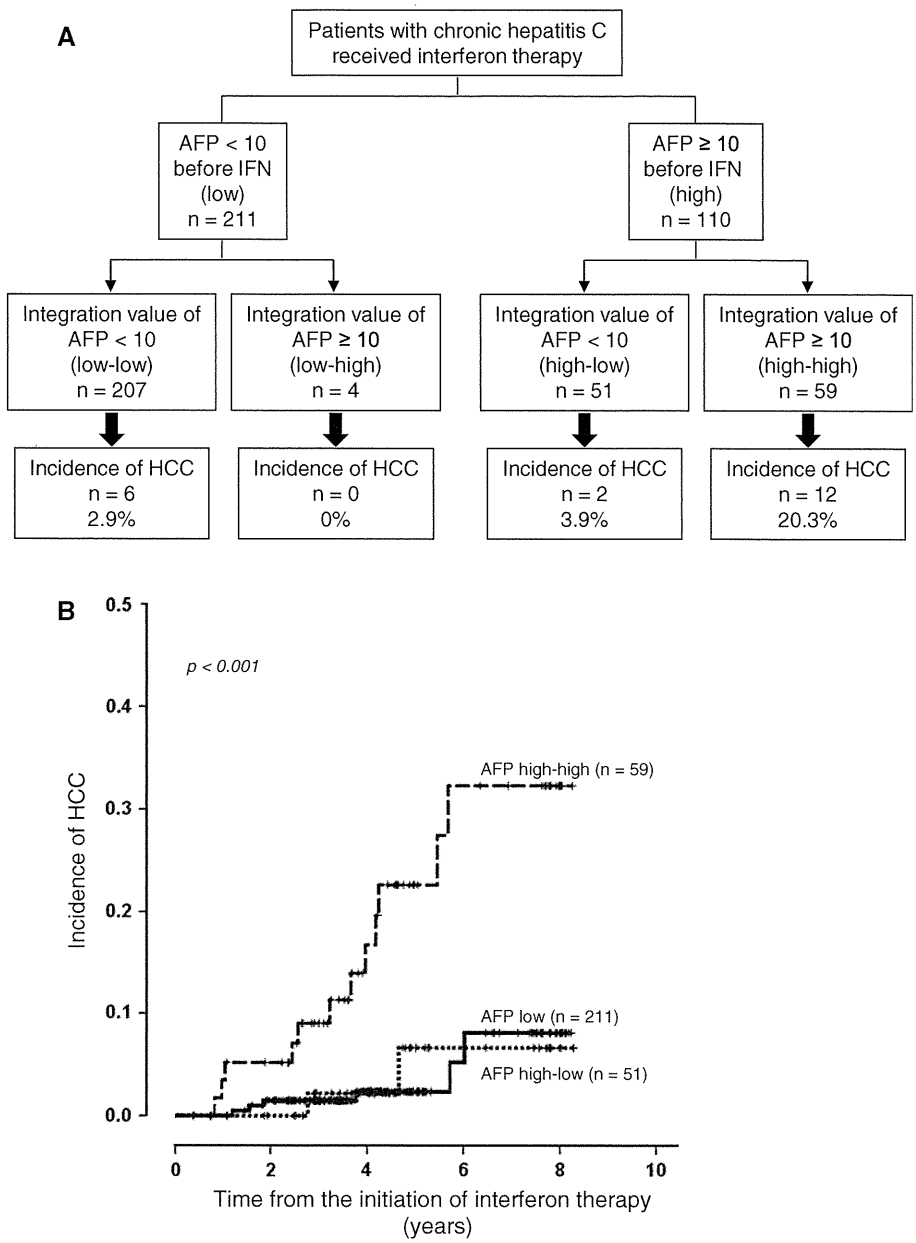

Fig. 3 AFP integration value as a predictive factor for HCC. **a** *Flow diagram* showing the number of patients (*n*) classified by baseline alpha-fetoprotein (AFP) levels before interferon (IFN) therapy and average AFP integration value, and the incidence of hepatocellular carcinoma (HCC) of each group. **b** Kaplan–Meier estimates of the incidence of HCC. *Solid line* AFP-low group (AFP levels before interferon therapy <10 ng/mL); *dotted line* AFP high–low group (baseline AFP levels ≥10 ng/mL, average AFP integration value <10 ng/mL); *dashed line* AFP high–high group (both baseline and average AFP integration values ≥10 ng/mL)

Data from several previous studies suggest that the continuous normalization of alanine aminotransferase (ALT) levels by interferon therapy can reduce the risk of HCC development [36–39]. In addition, one recent study suggested that the ALT integration value is a predictive factor for HCC [35]. In contrast to published data (22), our multivariate analysis did not identify the ALT integration value as a significant predictive factor for HCC incidence, although it was identified as significant by univariate analysis in all 382 patients. Since the previous study did not evaluate AFP levels as a factor for prediction of HCC [35], our results indicate that the AFP integration value is superior to that of ALT as a predictive factor for incidence of HCC. We do not know the reason for this result, but it is speculated that significance of AFP as a marker of hepatic regeneration resulted in the more accurate prediction of hepatocarcinogenesis by integration value of AFP than that of ALT.

As AFP is a diagnostic marker for the existence of HCC, high integration value of AFP in the present study might be a result of HCC development. However, we concluded that the high AFP integration values in patients who developed HCC were not caused by a result of existence of HCC, because of the following two reasons. First, the last AFP values before detection of HCC were not the highest level in the follow-up periods in 19 of 23 patients who developed

HCC, suggesting that the AFP was not produced by the developing HCC in these patients. Second, to exclude the influence of the remaining four patients whose last AFP levels were the highest in the follow-up periods, we analyzed the same statistical analysis by using average AFP integration values excluded the last two examinations of AFP before the detection of HCC. The results of the analysis also showed average integration value of AFP as a significant predictive factor for incidence of HCC.

Male gender was also identified as an independent risk factor for HCC in non-SVR patients in this study. Several reports have shown that men are at a higher risk of developing HCC than women [6, 10, 33, 40, 41]. The male gender also appears to be a risk factor for more severe disease and a greater risk of developing cirrhosis in chronic hepatitis C [42]. Although the association of male gender with the risk of HCC is as yet unexplained, hormonal or genetic factors may lead to increased risk for HCC and cirrhosis in men as previously discussed [10].

In conclusion, a decrease in the AFP integration value predicts reduced incidence of HCC in patients with hepatitis C receiving interferon therapy. Further prospective studies with a larger number of patients are required to validate the significance of these findings.

Acknowledgments This work was supported by Grants-in-aid for Scientific Research from the Ministry of Education, Culture, Sports, Science and Technology, and the Ministry of Health, Labor and Welfare of Japan.

Conflict of interest The authors declare that they have no conflict of interest.

References

1. Bruix J, Barrera JM, Calvet X, Ercilla G, Costa J, Sanchez-Tapias JM, Ventura M, Vall M, Bruguera M, Bru C, et al. Prevalence of antibodies to hepatitis C virus in Spanish patients with hepatocellular carcinoma and hepatic cirrhosis. Lancet. 1989;2:1004–6.
2. Colombo M, Kuo G, Choo QL, Donato MF, Del Ninno E, Tommasini MA, Dioguardi N, Houghton M. Prevalence of antibodies to hepatitis C virus in Italian patients with hepatocellular carcinoma. Lancet. 1989;2:1006–8.
3. Hasan F, Jeffers LJ, De Medina M, Reddy KR, Parker T, Schiff ER, Houghton M, Choo QL, Kuo G. Hepatitis C-associated hepatocellular carcinoma. Hepatology. 1990;12:589–91.
4. Ikeda K, Saitoh S, Koida I, Arase Y, Tsubota A, Chayama K, Kumada H, Kawanishi M. A multivariate analysis of risk factors for hepatocellular carcinogenesis: a prospective observation of 795 patients with viral and alcoholic cirrhosis. Hepatology. 1993;18:47–53.
5. Tsukuma H, Hiyama T, Tanaka S, Nakao M, Yabuuchi T, Kitamura T, Nakanishi K, Fujimoto I, Inoue A, Yamazaki H, et al. Risk factors for hepatocellular carcinoma among patients with chronic liver disease. N Engl J Med. 1993;328:1797–801.
6. Fattovich G, Stroffolini T, Zagni I, Donato F. Hepatocellular carcinoma in cirrhosis: incidence and risk factors. Gastroenterology. 2004;127:S35–50.
7. Ikeda K, Marusawa H, Osaki Y, Nakamura T, Kitajima N, Yamashita Y, Kudo M, Sato T, Chiba T. Antibody to hepatitis B core antigen and risk for hepatitis C-related hepatocellular carcinoma: a prospective study. Ann Intern Med. 2007;146:649–56.
8. Liang TJ, Heller T. Pathogenesis of hepatitis C-associated hepatocellular carcinoma. Gastroenterology. 2004;127:S62–71.
9. Yoshida H, Shiratori Y, Moriyama M, Arakawa Y, Ide T, Sata M, Inoue O, Yano M, Tanaka M, Fujiyama S, Nishiguchi S, Kuroki T, Imazeki F, Yokosuka O, Kinoyama S, Yamada G, Omata M. Interferon therapy reduces the risk for hepatocellular carcinoma: national surveillance program of cirrhotic and noncirrhotic patients with chronic hepatitis C in Japan. IHIT Study Group. Inhibition of hepatocarcinogenesis by interferon therapy. Ann Intern Med. 1999;131:174–81.
10. Heathcote EJ. Prevention of hepatitis C virus-related hepatocellular carcinoma. Gastroenterology. 2004;127:S294–302.
11. Lok AS, Seeff LB, Morgan TR, di Bisceglie AM, Sterling RK, Curto TM, Everson GT, Lindsay KL, Lee WM, Bonkovsky HL, Dienstag JL, Ghany MG, Morishima C, Goodman ZD. Incidence of hepatocellular carcinoma and associated risk factors in hepatitis C-related advanced liver disease. Gastroenterology. 2009; 136:138–48.
12. Effect of interferon-alpha on progression of cirrhosis to hepatocellular carcinoma: a retrospective cohort study. International Interferon-alpha Hepatocellular Carcinoma Study Group. Lancet. 1998;351:1535–9.
13. Camma C, Giunta M, Andreone P, Craxi A. Interferon and prevention of hepatocellular carcinoma in viral cirrhosis: an evidence-based approach. J Hepatol. 2001;34:593–602.
14. Di Bisceglie AM, Shiffman ML, Everson GT, Lindsay KL, Everhart JE, Wright EC, Lee WM, Lok AS, Bonkovsky HL, Morgan TR, Ghany MG, Morishima C, Snow KK, Dienstag JL. Prolonged therapy of advanced chronic hepatitis C with low-dose peginterferon. N Engl J Med. 2008;359:2429–41.
15. Fattovich G, Giustina G, Degos F, Diodati G, Tremolada F, Nevens F, Almasio P, Solinas A, Brouwer JT, Thomas H, Realdi G, Corrocher R, Schalm SW. Effectiveness of interferon alfa on incidence of hepatocellular carcinoma, decompensation in cirrhosis type C. European Concerted Action on Viral Hepatitis (EUROHEP). J Hepatol. 1997;27:201–5.
16. Hayashi K, Kumada T, Nakano S, Takeda I, Kiriyama S, Sone Y, Toyoda H, Shimizu H, Honda T. Incidence of hepatocellular carcinoma in chronic hepatitis C after interferon therapy. Hepatogastroenterology. 2002;49:508–12.
17. Lok AS, Everhart JE, Wright EC, Di Bisceglie AM, Kim HY, Sterling RK, Everson GT, Lindsay KL, Lee WM, Bonkovsky HL, Dienstag JL, Ghany MG, Morishima C, Morgan TR. Maintenance peginterferon therapy and other factors associated with hepatocellular carcinoma in patients with advanced hepatitis C. Gastroenterology. 2011;140:840–9.
18. Nishiguchi S, Kuroki T, Nakatani S, Morimoto H, Takeda T, Nakajima S, Shiomi S, Seki S, Kobayashi K, Otani S. Randomised trial of effects of interferon-alpha on incidence of hepatocellular carcinoma in chronic active hepatitis C with cirrhosis. Lancet. 1995;346:1051–5.
19. Okanoue T, Itoh Y, Minami M, Sakamoto S, Yasui K, Sakamoto M, Nishioji K, Murakami Y, Kashima K. Interferon therapy lowers the rate of progression to hepatocellular carcinoma in chronic hepatitis C but not significantly in an advanced stage: a retrospective study in 1148 patients. Viral Hepatitis Therapy Study Group. J Hepatol. 1999;30:653–9.
20. Izuno K, Fujiyama S, Yamasaki K, Sato M, Sato T. Early detection of hepatocellular carcinoma associated with cirrhosis by combined assay of des-gamma-carboxy prothrombin and alpha-fetoprotein: a prospective study. Hepatogastroenterology. 1995;42:387–93.

21. Trevisani F, D'Intino PE, Morselli-Labate AM, Mazzella G, Accogli E, Caraceni P, Domenicali M, De Notariis S, Roda E, Bernardi M. Serum alpha-fetoprotein for diagnosis of hepatocellular carcinoma in patients with chronic liver disease: influence of HBsAg and anti-HCV status. J Hepatol. 2001;34:570–5.
22. Zoli M, Magalotti D, Bianchi G, Gueli C, Marchesini G, Pisi E. Efficacy of a surveillance program for early detection of hepatocellular carcinoma. Cancer. 1996;78:977–85.
23. Alpert E, Feller ER. Alpha-fetoprotein (AFP) in benign liver disease. Evidence that normal liver regeneration does not induce AFP synthesis. Gastroenterology. 1978;74:856–8.
24. Bloomer JR, Waldmann TA, McIntire KR, Klatskin G. Alpha-fetoprotein in noneoplastic hepatic disorders. JAMA. 1975;233: 38–41.
25. Ruoslahti E, Seppala M. Normal and increased alpha-fetoprotein in neoplastic and non-neoplastic liver disease. Lancet. 1972;2: 278–9.
26. Sakurai T, Marusawa H, Satomura S, Nabeshima M, Uemoto S, Tanaka K, Chiba T. *Lens culinaris* agglutinin-A-reactive alpha-fetoprotein as a marker for liver atrophy in fulminant hepatic failure. Hepatol Res. 2003;26:98–105.
27. Taketa K. Alpha-fetoprotein: reevaluation in hepatology. Hepatology. 1990;12:1420–32.
28. Di Bisceglie AM, Sterling RK, Chung RT, Everhart JE, Dienstag JL, Bonkovsky HL, Wright EC, Everson GT, Lindsay KL, Lok AS, Lee WM, Morgan TR, Ghany MG, Gretch DR. Serum alpha-fetoprotein levels in patients with advanced hepatitis C: results from the HALT-C Trial. J Hepatol. 2005;43:434–41.
29. Tateyama M, Yatsuhashi H, Taura N, Motoyoshi Y, Nagaoka S, Yanagi K, Abiru S, Yano K, Komori A, Migita K, Nakamura M, Nagahama H, Sasaki Y, Miyakawa Y, Ishibashi H. Alpha-fetoprotein above normal levels as a risk factor for the development of hepatocellular carcinoma in patients infected with hepatitis C virus. J Gastroenterol. 2011;46:92–100.
30. Murashima S, Tanaka M, Haramaki M, Yutani S, Nakashima Y, Harada K, Ide T, Kumashiro R, Sata M. A decrease in AFP level related to administration of interferon in patients with chronic hepatitis C and a high level of AFP. Dig Dis Sci. 2006;51: 808–12.
31. Tamura Y, Yamagiwa S, Aoki Y, Kurita S, Suda T, Ohkoshi S, Nomoto M, Aoyagi Y. Serum alpha-fetoprotein levels during and after interferon therapy and the development of hepatocellular carcinoma in patients with chronic hepatitis C. Dig Dis Sci. 2009;54:2530–7.
32. Arase Y, Ikeda K, Suzuki F, Suzuki Y, Kobayashi M, Akuta N, Hosaka T, Sezaki H, Yatsuji H, Kawamura Y, Kumada H. Prolonged-interferon therapy reduces hepatocarcinogenesis in aged-patients with chronic hepatitis C. J Med Virol. 2007;79: 1095–102.
33. Asahina Y, Tsuchiya K, Tamaki N, Hirayama I, Tanaka T, Sato M, Yasui Y, Hosokawa T, Ueda K, Kuzuya T, Nakanishi H, Itakura J, Takahashi Y, Kurosaki M, Enomoto N, Izumi N. Effect of aging on risk for hepatocellular carcinoma in chronic hepatitis C virus infection. Hepatology. 2010;52:518–27.
34. Ohno O, Mizokami M, Wu RR, Saleh MG, Ohba K, Orito E, Mukaide M, Williams R, Lau JY. New hepatitis C virus (HCV) genotyping system that allows for identification of HCV genotypes 1a, 1b, 2a, 2b, 3a, 3b, 4, 5a, and 6a. J Clin Microbiol. 1997;35:201–7.
35. Kumada T, Toyoda H, Kiriyama S, Sone Y, Tanikawa M, Hisanaga Y, Kanamori A, Atsumi H, Takagi M, Nakano S, Arakawa T, Fujimori M. Incidence of hepatocellular carcinoma in hepatitis C carriers with normal alanine aminotransferase levels. J Hepatol. 2009;50:729–35.
36. Arase Y, Ikeda K, Suzuki F, Suzuki Y, Kobayashi M, Akuta N, Hosaka T, Sezaki H, Yatsuji H, Kawamura Y, Kumada H. Interferon-induced prolonged biochemical response reduces hepatocarcinogenesis in hepatitis C virus infection. J Med Virol. 2007;79:1485–90.
37. Kasahara A, Hayashi N, Mochizuki K, Takayanagi M, Yoshioka K, Kakumu S, Iijima A, Urushihara A, Kiyosawa K, Okuda M, Hino K, Okita K. Risk factors for hepatocellular carcinoma, its incidence after interferon treatment in patients with chronic hepatitis C. Osaka Liver Disease Study Group. Hepatology. 1998;27:1394–402.
38. Kurokawa M, Hiramatsu N, Oze T, Mochizuki K, Yakushijin T, Kurashige N, Inoue Y, Igura T, Imanaka K, Yamada A, Oshita M, Hagiwara H, Mita E, Ito T, Inui Y, Hijioka T, Yoshihara H, Inoue A, Imai Y, Kato M, Kiso S, Kanto T, Takehara T, Kasahara A, Hayashi N. Effect of interferon alpha-2b plus ribavirin therapy on incidence of hepatocellular carcinoma in patients with chronic hepatitis. Hepatol Res. 2009;39:432–8.
39. Suzuki K, Ohkoshi S, Yano M, Ichida T, Takimoto M, Naitoh A, Mori S, Hata K, Igarashi K, Hara H, Ohta H, Soga K, Watanabe T, Kamimura T, Aoyagi Y. Sustained biochemical remission after interferon treatment may closely be related to the end of treatment biochemical response and associated with a lower incidence of hepatocarcinogenesis. Liver Int. 2003;23:143–7.
40. Kurosaki M, Hosokawa T, Matsunaga K, Hirayama I, Tanaka T, Sato M, Yasui Y, Tamaki N, Ueda K, Tsuchiya K, Kuzuya T, Nakanishi H, Itakura J, Takahashi Y, Asahina Y, Enomoto N, Izumi N. Hepatic steatosis in chronic hepatitis C is a significant risk factor for developing hepatocellular carcinoma independent of age, sex, obesity, fibrosis stage and response to interferon therapy. Hepatol Res. 2010;40:870–7.
41. Takahashi H, Mizuta T, Eguchi Y, Kawaguchi Y, Kuwashiro T, Oeda S, Isoda H, Oza N, Iwane S, Izumi K, Anzai K, Ozaki I, Fujimoto K. Post-challenge hyperglycemia is a significant risk factor for the development of hepatocellular carcinoma in patients with chronic hepatitis C. J Gastroenterol. 2011;46:790–8.
42. Forns X, Ampurdanes S, Sanchez-Tapias JM, Guilera M, Sans M, Sanchez-Fueyo A, Quinto L, Joya P, Bruguera M, Rodes J. Long-term follow-up of chronic hepatitis C in patients diagnosed at a tertiary-care center. J Hepatol. 2001;35:265–71.

Case Reports in Gastroenterology

Case Rep Gastroenterol 2011;5:100–109
DOI: 10.1159/000326951

Published online: March 26, 2011

ISSN 1662–0631
www.karger.com/crg

Drinking Status of Heavy Drinkers Detected by Arrival Time Parametric Imaging Using Sonazoid-Enhanced Ultrasonography: Study of Two Cases

Noritaka Wakui[a] Ryuji Takayama[a] Takahiko Mimura[a]
Naohisa Kamiyama[c] Kenichi Maruyama[b] Yasukiyo Sumino[a]

[a]Division of Gastroenterology and Hepatology and [b]Division of Clinical Functional Physiology, Toho University Omori Medical Center, Tokyo, and [c]The Ultrasound Systems, Development Department, Toshiba Medical Systems Corporation, Otawara, Japan

Key Words
Alcoholic liver disease · Contrast-enhanced ultrasonography · Arrival time parametric imaging · Sonazoid · Liver

Abstract
Chronic heavy consumption of alcohol is associated with increased risks of developing liver cirrhosis, hepatocellular carcinoma, and esophageal varices. Cessation of alcohol consumption is the most important requirement in treating these diseases. However, judging whether patients have actually maintained abstinence from alcohol requires reliance on their reports, which vary substantially across individuals using the test methods currently available. Arrival time parametric imaging (At-PI) using Sonazoid-enhanced ultrasonography is regarded as a useful approach for assessing the progression of lesions that have developed in liver parenchyma. In this study, we report two cases for whom this approach was successfully applied to indicate the drinking status of a heavy drinker. At-PI enables approximate and objective assessment of the drinking status of patients, independent of their reports; therefore, it is a promising method for providing information about drinking status.

Introduction

In Japan, alcoholic drinks have been consumed during ceremonies since ancient times and have became popular as grocery items among the general public. However, chronic heavy consumption of alcohol can induce alcoholic liver disease that may progress to liver

Noritaka Wakui, MD, PhD
Division of Gastroenterology and Hepatology, Toho University Omori Medical Center
6-11-1 Omori-nishi, Ota-ku, Tokyo 143-8541 (Japan)
Tel. +81 3 3762 4151, E-Mail toho_med_wakui@yahoo.co.jp

cirrhosis, which in turn leads to increased incidence of esophageal varices and hepatocellular carcinoma [1–3]. Prognosis of alcoholic liver cirrhosis induced by excessive consumption of alcohol is poor, and the 5-year survival rate was reported to be 40.5% [4]. On the other hand, it is known that successful cessation of alcohol consumption markedly ameliorates liver cirrhosis [5, 6]. Therefore, patient commitment to remaining abstinent from alcohol is the ultimate determinant of prognosis for this disease. Moreover, reversibility of hepatic fibrosis has been proven histologically [7], and long-term abstinence from alcohol has been reported to reduce pre-existing fibrosis, which consequently decreases portal pressure, leading to a possible amelioration of esophageal varices [8].

During medical consultations, however, patients often deny or conceal the fact that they are regularly consuming alcohol, and the information they provide regarding their alcohol consumption habits tends to be inaccurate. To overcome this problem, the ratio of asparate aminotransferase to alanine aminotransferase (AST/ALT ratio), gamma-glutamyl transpeptidase (γ-GTP) activity, and the level of IgA were suggested as indicators of drinking status since they play a role in diagnosing alcoholic liver cirrhosis [9–13]. However, measuring these indicators does not provide conclusive evidence of drinking status because the magnitude of changes in these measurements varies considerably across individuals [11–13]. This means that accurate understanding of patients' drinking status is still dependent on their reports. Therefore, a different approach that enables objective assessment of drinking status will be of great benefit in daily clinical practice.

Arrival time parametric imaging (At-PI) using Sonazoid-enhanced ultrasonography is regarded as a useful approach for assessing the progression of lesions that have developed in liver parenchyma. In this study, we employed this approach to assess the drinking status of two heavy drinkers. We report interesting findings when comparing patients' drinking status as indicated by At-PI-based laboratory test results against their reports.

Case Report

Liver Parenchyma Blood Flow Imaging

A Toshiba SSA-790 system (Aplio XG; Toshiba Medical Systems, Otawara, Japan) with a 3.75 MHz convex array probe (PVT-375BT; Toshiba Medical Systems) was used for blood flow imaging. The system was operated at a mechanical index of 0.22–0.29 and a frame rate of 15–18 frames/s, and right intercostal images were acquired to view the liver and kidney on the same screen simultaneously. The focal depth was adjusted within a range of 6–8 cm depending on the thickness of the kidney. Then, the recommended amount (0.015 ml/kg) of Sonazoid (perfluorobutane; GE Healthcare, Oslo, Norway) was injected into the antecubital vein. Imaging was started immediately after injection for a period of approximately 40 s, and the acquired images were stored as raw data in the system hardware.

At-PI

To study the kinetics of the ultrasound signals, arrival time parametric images of the liver parenchyma were constructed from ultrasound raw data using a software program (At-PI; Toshiba Medical Systems) that interfaced with the ultrasound system. Briefly, the stored video was started after selecting the region of interest within the kidney parenchyma on a still image. Construction of an arrival time parametric image was started automatically when the signal intensity exceeded the set level in 80% of the region of interest. The time interval from the start of the construction (time 0) to the appearance

of contrast (arrival time) in individual pixels of the liver parenchyma imaging agent was depicted using multiple colors for different arrival times as follows: red 0–1 s; orange 1–2 s; yellow 2–3 s; light green 3–4 s; dark green 4–5 s; light blue 5–6 s; dark blue 6 s or longer (fig. 1). This study was approved by the institutional ethics committee, and informed consent was obtained from the patients.

Case 1

Case 1 was a 60-year-old male who managed a bar and had been drinking heavily for 20 years. He consumed 2 mid-sized glasses of beer and 10 glasses of shochu liquor mixed with warm water on a daily basis (effective ethanol consumption: 200 g/day). After liver dysfunction was indicated by a blood test performed as part of a health checkup, he visited Toho University Omori Medical Center in April 2009. Laboratory findings on admission were: ammonia (NH_3) 78 μg/dl; albumin (Alb) 2.8 g/dl; total bilirubin (T-bil) 1.4 mg/dl; direct bilirubin (D-bil) 0.7 mg/dl; AST 102 IU/l; ALT 45 IU/l; lactate dehydrogenase (LDH) 329 IU/l; alkaline phosphatase (ALP) 331 IU/l; γ-GTP 266 IU/l; cholinesterase (ChE) 96 IU/l; platelets (Plt) 40×10^4/μl; prothrombin time (PT) 45%; antibodies to hepatitis C virus (HCVAb) negative; hepatitis B surface antigen (HBsAg) negative; antibodies to hepatitis B surface antigen (HBsAb) negative. These findings indicated elevation of transaminase levels with AST dominance and deterioration of liver function.

The patient tried to remain abstinent from alcohol and follow-up laboratory tests showed that levels of AST, ALT, γ-GTP, and PT had improved to 24, 27, and 136 IU/l and 71%, respectively, in December 2009, and further to 21, 21, and 104 IU/l and 75%, respectively, in July 2010 (table 1). At-PI results in April 2009, December 2009, and July 2010 are shown in figure 2, figure 3 and figure 4, respectively. Red, indicative of early arrival time, was the dominant color in the entire region of the arrival time parametric image of the liver taken in April 2009, while blue, indicative of late arrival time, was more dominant in more recent images. In other words, it was suggested that blood flow to the liver had slowed during the follow-up period.

Case 2

Case 2 was a 51-year-old patient with liver damage who was referred to Toho University Omori Medical Center by a local physician in March 2010. He had been consuming 900 ml of shochu liquor on a daily basis for 30 years (effective ethanol consumption: 225 g/day). Laboratory findings on admission were: NH_3 24 μg/dl; Alb 1.8 g/dl; T-bil 2.4 mg/dl; D-bil 1.4 mg/dl; AST 53 IU/l; ALT 13 IU/l; LDH 219 IU/l; ALP 922 IU/l; γ-GTP 658 IU/l; ChE 80 IU/l; Plt 41×10^4/μl; PT 33%; HCVAb negative; HBsAg negative; HBsAb negative. These findings indicated elevation of transaminase levels with AST dominance and deterioration of liver function. Red, indicative of early arrival time, was the dominant color in the entire region of the arrival time parametric image of the liver constructed from Sonazoid-enhanced ultrasound results (fig. 5).

The first follow-up examination was performed in May 2010. The patient reported that he had remained abstinent from alcohol and laboratory tests showed that levels of AST, ALT, γ-GTP, and PT had improved to 21, 5, and 157 IU/l and 46%, respectively (table 2). At-PI showed that yellow, indicating an arrival time of 2–3 s, had increased (fig. 6), suggesting that blood flow into the liver had slowed. The second follow-up examination was performed in July 2010, and the patient reported that he had not consumed alcohol since the previous examination. Laboratory tests showed an increase in PT (63%), suggesting liver function improvement, while levels of AST, ALT, and γ-GTP were not improved, but elevated to 53, 13, and 408 IU/l, respectively (table 2). The arrival time parametric image of the entire liver had reverted to a red-dominated image, suggesting that the blood flow into the liver had improved (fig. 7). The patient was re-questioned about his recent drinking status while presenting the At-PI results. His answers revealed that he had resumed drinking 1 month earlier and has been consuming 900 ml of shochu liquor on a daily basis (effective ethanol consumption: 225 g/day).

Discussion

The liver receives a dual blood supply from the hepatic portal vein and hepatic arteries, both of which drain blood into the hepatic vein via the liver sinusoids. It is understood that both the former and latter deliver a crucial supply of blood to the hepatocytes and cholangiocytes, respectively. In healthy individuals, the hepatic portal vein and hepatic arteries supply approximately 80 and 20% of liver blood, respectively [14]. In patients with viral hepatitis, this balance is altered toward arterial supply in line with the progression of chronic hepatitis to hepatic cirrhosis, since necrosis and loss of hepatocytes occur, which subsequently causes changes such as regeneration of liver tissue and fibrosis [14–17].

On the other hand, in patients with alcoholic liver disease induced by heavy drinking, elevation of portal venous pressure is seen even though the disease has not yet progressed to hepatic cirrhosis. Thickening of the central venous wall has been suggested as a potential reason for this pressure increase [18], and a mechanism involving the direct action of alcohol on collagen metabolism, independent of fibrosis caused by necrosis and inflammation, was proposed [19]. Changes associated with acute alcoholic hepatitis appear reversible. Necrosis and inflammatory cell infiltration induced by a large consumption of alcohol were reduced by the end of the fourth week of abstinence from alcohol, and deposition of basement membrane components including type IV collagen and laminin in the sinusoids was reduced, while histological findings characteristic of alcoholic hepatitis, such as expression of factor VIII-related antigen in sinusoidal endothelial cells, disappeared approximately 10 weeks after cessation of alcohol consumption [20]. Taken together, continuous heavy drinking elevates portal venous pressure which disturbs the normal balance of the dual blood supply to the liver (portal venous flow:arterial flow = 8:2). In response, the arterial flow increases to compensate for the decreased portal venous flow, and consequently, the blood supply balance shifts toward arterial domination [15]. Furthermore, this altered balance can be reverted to portal venous domination by abstaining from drinking.

At-PI is an ultrasound image analysis tool that monitors the intensity of ultrasound signals over time and presents color-coded images converted from sequential raw data. The At-PI-based approach used in this study is based on the relative time taken for blood flow to arrive at the liver compared to that of the kidney. The kidney receives blood from only the renal arteries, while the liver receives blood from both the hepatic portal vein and hepatic arteries; this difference is the reason why time 0 of At-PI of the liver is set as the arrival time of a contrast agent into the kidney. Chronic heavy drinking alters the hepatic blood supply balance from portal venous flow to arterial flow, and this imbalance can be predicted by studying the interval between the arrival time of the blood flow to the kidney (via the arterial route) and that to the liver. In other words, when the interval becomes shorter, the dominant source of the ultrasound signals in the liver is thought to arise more from the arterial flow than from the portal venous flow. Therefore, this approach enables objective assessment of blood supply balance between the hepatic portal venous flow and arterial flow.

When studying the balance of the dual blood supply system of the liver, the interval between the arrival time of blood flow to the liver parenchyma via the portal vein and that via the arteries is another important factor because it indicates roughly the dominant supply route: the hepatic portal venous route or arterial route. In healthy individuals, the

arrival time interval is reported to be approximately 5–6 s [21]. With respect to the color code used in this study, arrival time parametric color images dominated by light and dark blue (arrival time interval of 5 s or longer) can be interpreted as indicating that the portal vein is the main route of blood flow to the liver parenchyma. Light and dark blue-colored liver images also suggest the possibility that the blood supply condition is similar to that of a healthy individual; in other words, patients have successfully remained abstinent from alcohol or reduced consumption of alcohol. Conversely, red-dominated liver images suggest the possibility that the patient continued drinking heavily.

When the results of case 1 were assessed according to the above-mentioned color-based system, the initial red-dominated image, taken at the time the patient was drinking heavily and indicative of the dominance of arterial blood supply to the liver parenchyma, changed to a blue-dominated image after cessation of alcohol consumption, suggesting that the slow velocity flow, namely the hepatic portal venous flow, became the dominant supply to the liver. Similarly, the initial red-dominated image of case 2 became more yellow after cessation of alcohol consumption. However, this sign of improvement reverted to the previous state, and most of the arrival time parametric image became red upon reintroduction of alcohol.

The results revealed that At-PI of liver parenchyma provides easy-to-understand color-coded visual information regarding the balance between hepatic arterial flow and portal venous flow. Moreover, because this approach enables objective assessment of the drinking status of patients on the basis of one final still image, it provided convincing evidence to the patient in case 2, whose laboratory test results had been contradicted by his self-reported status of alcohol consumption, to abstain from consuming alcohol. However, this approach does not provide quantitative information on the amount of alcohol consumed, and its application is currently limited to comparative assessment between two examinations performed on different dates, whereby only an increase or decrease in alcohol consumption is indicated. Development of a new approach enabling quantitative assessment of alcohol consumption is anticipated in the future. Nevertheless, considering that At-PI offers objective data indicating approximate alcohol consumption status, independent of the reports made by patients, it is suggested that arrival time parametric image will become a powerful indicator of alcohol consumption.

Table 1. Case 1

	April 2009	December 2009	July 2010
NH_3, μg/dl	78	57	55
Alb, g/dl	2.8	3.7	3.9
T-bil, mg/dl	1.4	0.8	0.7
D-bil, mg/dl	0.7	0.2	0.1
AST, IU/l	102	24	21
ALT, IU/l	45	27	21
LDH, IU/l	329	183	172
ALP, IU/l	331	462	390
γ-GTP, IU/l	266	136	104
ChE, IU/l	96	249	259
Plt, $\times 10^4$/μl	40	17.8	18.8
PT, %	45	71	75
HCVAb	(–)		
HBsAg	(–)		
HBsAb	(–)		

Table 2. Case 2

	March 2010	May 2010	July 2010
NH_3, μg/dl	24	–	–
Alb, g/dl	1.8	3.4	4.3
T-bil, mg/dl	2.4	1.7	2.9
D-bil, mg/dl	1.4	0.7	1.5
AST, IU/l	53	21	53
ALT, IU/l	13	5	13
LDH, IU/l	219	140	199
ALP, IU/l	922	258	359
γ-GTP, IU/l	658	157	408
ChE, IU/l	80	194	27
Plt, $\times 10^4$/μl	41	21	10.5
PT, %	33	46	63
HCVAb	(–)		
HBsAg	(–)		
HBsAb	(–)		

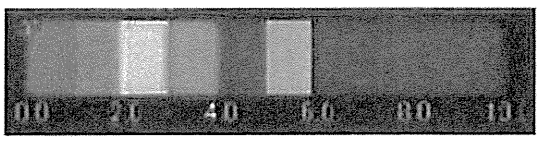

Fig. 1. Colors used in arrival time parametric images and the corresponding arrival times for the contrast agent to arrive in the liver are shown as follows: red 0–1 s; orange 1–2 s; yellow 2–3 s; light green 3–4 s; dark green 4–5 s; light blue 5–6 s; dark blue 6 s or longer.

Case Rep Gastroenterol 2011;5:100–109
DOI: 10.1159/000326951
Published online: March 26, 2011

ISSN 1662–0631
www.karger.com/crg

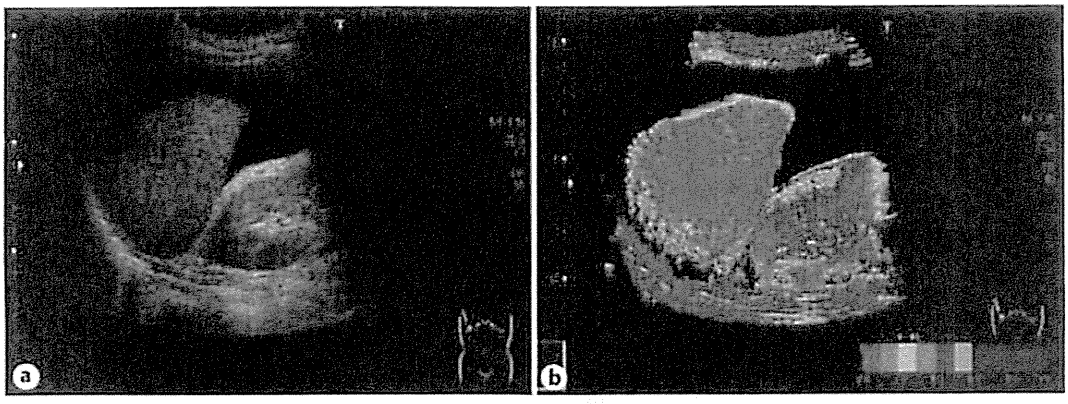

Fig. 2. Ultrasound images of case 1 taken in April 2009. **a** B-mode ultrasound image. **b** Arrival time parametric image. Red is dominant in the entire area of the arrival time parametric image of the liver.

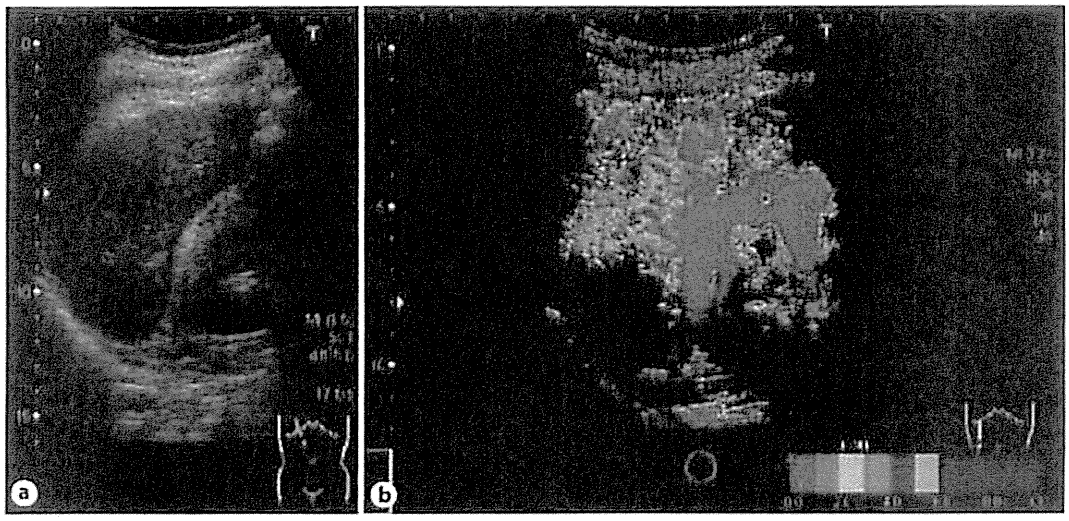

Fig. 3. Ultrasound images of case 1 taken in December 2009. **a** B-mode ultrasound image. **b** Arrival time parametric image. The red-colored region decreased, while light and dark green-colored regions increased in the entire area of the arrival time parametric image of the liver.

Case Rep Gastroenterol 2011;5:100–109
DOI: 10.1159/000326951
Published online: March 26, 2011

ISSN 1662–0631
www.karger.com/crg

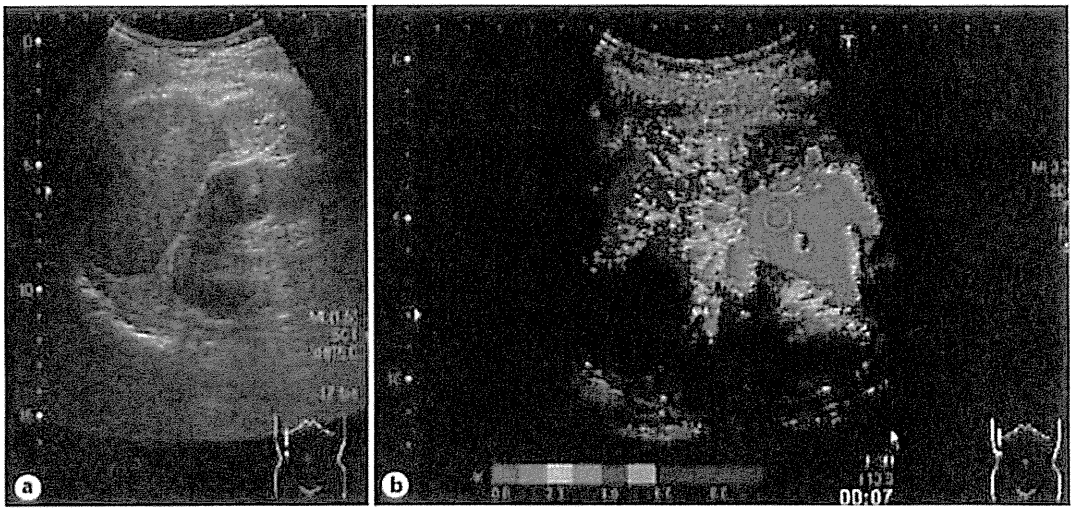

Fig. 4. Ultrasound images of case 1 taken in July 2010. **a** B-mode ultrasound image. **b** Arrival time parametric image. Blue, indicative of late arrival, dominated the entire area of the arrival time parametric image of the liver.

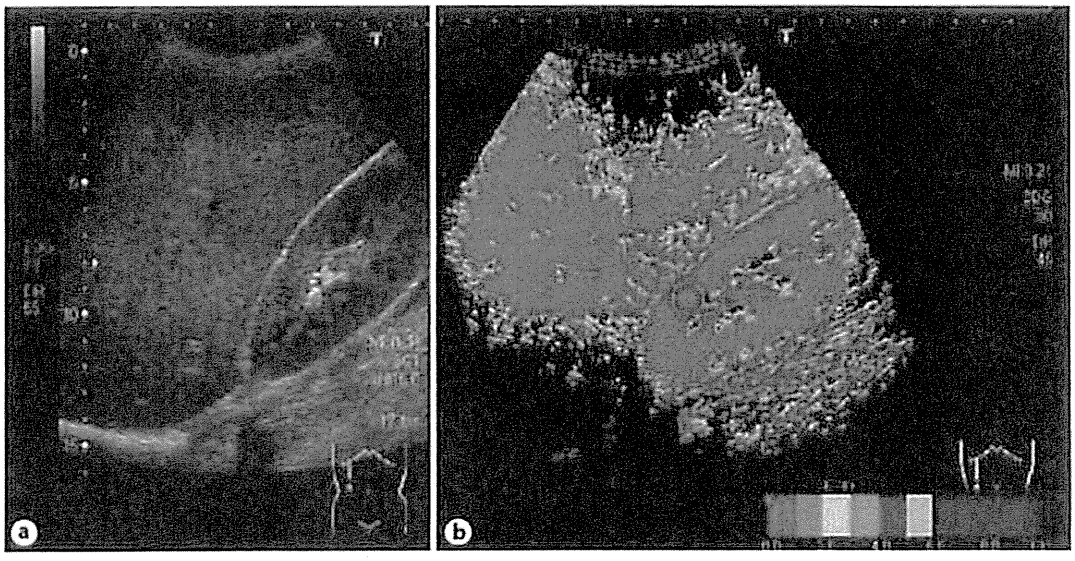

Fig. 5. Ultrasound images of case 2 taken in March 2010. **a** B-mode ultrasound image. **b** Arrival time parametric image. Red, indicative of early arrival, dominated the entire area of the arrival time parametric image of the liver.

Case Rep Gastroenterol 2011;5:100–109
DOI: 10.1159/000326951
Published online: March 26, 2011

ISSN 1662–0631
www.karger.com/crg

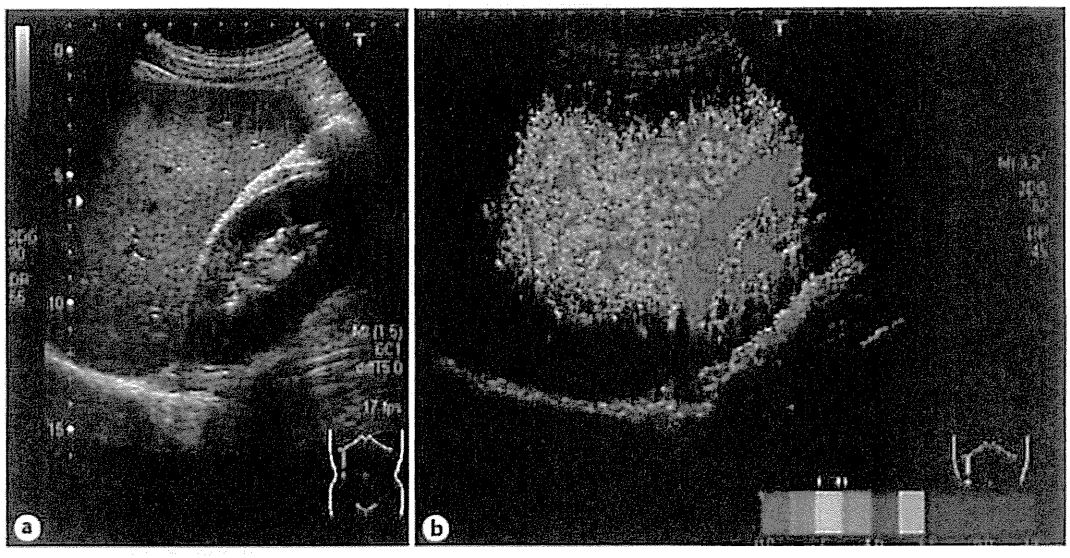

Fig. 6. Ultrasound images of case 2 taken in May 2010. **a** B-mode ultrasound image. **b** Arrival time parametric image. The red-colored region decreased, while yellow- and light green-colored regions increased in the entire area of the arrival time parametric image of the liver.

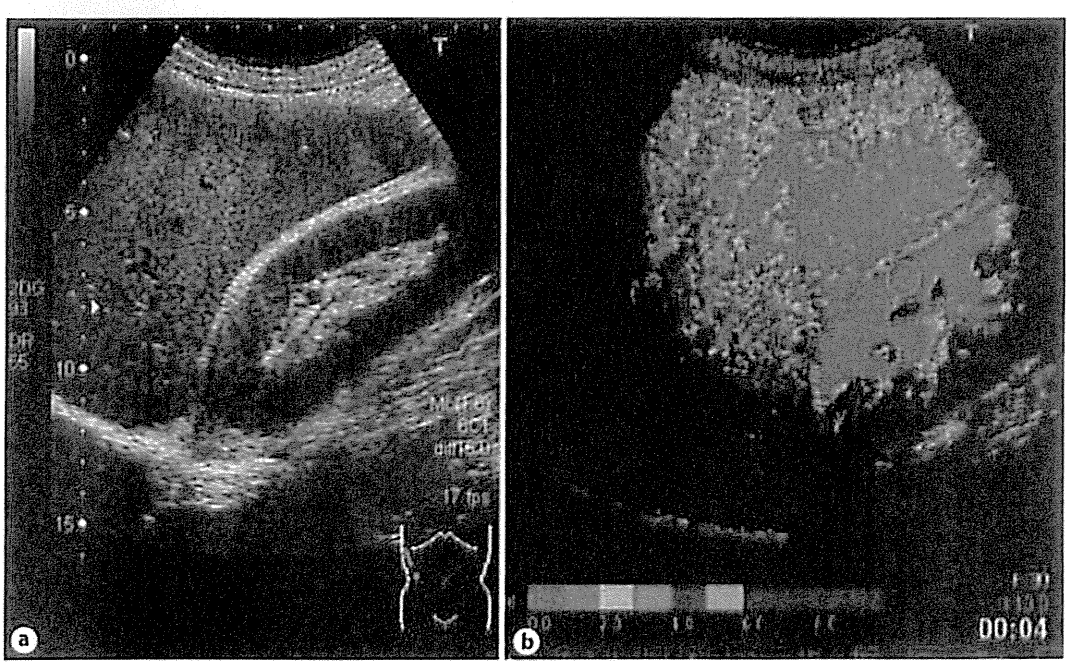

Fig. 7. Ultrasound images of case 2 taken in July 2010. **a** B-mode ultrasound image. **b** Arrival time parametric image. The ratio of the red-colored region, indicative of early arrival, increased for a second time in the entire area of the arrival time parametric image of the liver.

References

1 Tsutsumi M, Ishizaki M, Takada A: Relative risk for the development of hepatocellular carcinoma in alcoholic patients with cirrhosis: A multiple logistic regression coefficient analysis. Alcohol Clin Exp Res 1996;20:758–762.

2 Adachi M, Brenner DA: Clinical syndromes of alcoholic liver disease. Dig Dis 2005;23:255–263.

3 Tilg H, Day CP: Management strategies in alcoholic liver disease. Nat Clin Pract Gastroenterol Hepatol 2007;4:24–34.

4 Powell WJ, Klatskin G: Duration of survival in patients with Laennec's cirrhosis. Am J Med 1968;44:406–420.

5 Merkel C, Marchesini G, Fabbri A, et al: The course of galactose elimination capacity in patients with alcoholic cirrhosis: possible use as a surrogate marker for death. Hepatology 1996;24:820–823.

6 Yokoyama A, Matsushita S, Ishii H, et al: The impact of diabetes mellitus on the prognosis of alcoholics. Alcohol 1994;29:181–186.

7 Nakano M: Histological changes of alcoholic fibrosis after abstinence in baboon (in Japanese). Alcohol Biomed Res 1996;16:137–140.

8 Fujii M, Nakano S, Hachiya A: Abstinent efficacy estimated by hepatic function and portal venous pressure in liver cirrhosis (in Japanese). JJPH 2001;7:213–217.

9 Cohen JA, Kaplan MM: The SGOT/SGPT ratio – an indicator of alcoholic liver disease. Dig Dis Sci 1979;24: 835–838.

10 Matloff DS, Selinger MJ, Kaplan MM: Hepatic transaminase activity in alcoholic liver disease. Gastroenterology 1980;78:1389–1392.

11 Ishii H, Asuraoka S, Shigeta Y, et al: Hepatic and intestinal gamma-glutamyltranspeptidase activity: its activation by chronic ethanol administration. Life Sci 1978;23:1393–1397.

12 Morgan MY, Ross MG, Ng CM, et al: HLA-B8, immunoglobulins, and antibody responses in alcohol related liver disease. J Clin Pathol 1980;33:488–492.

13 Irie M, Suzuki N, Sohda T, et al: Hepatic expression of gamma-glutamyl transpeptidase in the human liver of patients with alcoholic liver disease. Hepatol Res 2007;37:966–973.

14 Kleber G, Steudel N, Behrmann C, et al: Hepatic arterial flow volume and reserve in patients with cirrhosis: use of intra-arterial Doppler and adenosine infusion. Gastroenterology 1999;116:906–914.

15 Rocheleau B, Ethier C, Houle R, et al: Hepatic artery buffer response following left portal vein ligation: its role in liver tissue homeostasis. Am J Physiol 1999;277:G1000–G1007.

16 Leen E, Goldberg JA, Anderson JR, et al: Hepatic perfusion changes in patients with liver metastases: comparison with those patients with cirrhosis. Gut 1993;34:554–557.

17 Lautt WW: Mechanism and role of intrinsic regulation of hepatic arterial blood flow: hepatic arterial buffer response. Am J Physiol 1985;249:G549–G556.

18 Edmondson HA, Peters RL, Reynolds TB, et al: Sclerosing hyaline necrosis of the liver in the chronic alcoholic: A recognizable clinical syndrome. Ann Intern Med 1963;59:646–673.

19 Popper H, Lieber CS: Die alkoholische Zirrhose folgt nicht notwendigerweise der Alkoholhepatitis. Internist (Berl) 1979;20:176–178.

20 Urashima S, Tsutsumi M, Nakase K, et al: Studies on capillarization of the hepatic sinusoids in alcoholic liver disease. Alcohol Alcohol Suppl 1993;1B:77–84.

21 Iijima H, Sasaki S, Moriyasu F, et al: Dynamic US contrast study of the liver: Vascular and delayed parenchymal phase. Hepatol Res 2007;37:27–34.

Hepatology Research

Hepatology Research 2011; 41: 375–385 doi: 10.1111/j.1872-034X.2010.00769.x

Original Article

Pitavastatin inhibits hepatic steatosis and fibrosis in non-alcoholic steatohepatitis model rats

Tomokatsu Miyaki,[1] Shunsuke Nojiri,[1] Noboru Shinkai,[1] Atsunori Kusakabe,[1] Kentaro Matsuura,[1] Etsuko Iio,[1] Satoru Takahashi,[2] Ge Yan,[3] Kazuo Ikeda[3] and Takashi Joh[1]

Departments of [1]Gastroenterology and Metabolism, [2]Experimental Pathology and Tumor Biology, and [3]Cell Biology and Anatomy, Nagoya City University Graduate School of Medical Sciences, Nagoya, Aichi, Japan

Aim: Non-alcoholic steatohepatitis (NASH) may progress to liver cirrhosis, and NASH patients with liver cirrhosis are at risk of developing hepatocellular carcinoma. Statins, 3-hydroxy-3-methyglutaryl-coenzyme A reductase inhibitors, are well known to reduce low-density lipoprotein cholesterol and reduce the incidence of coronary heart disease and other major vascular events by anti-inflammatory and antifibrotic effects, and antiproliferative properties in colorectal cancers have also been reported. Recently, statins have been reported to improve hepatic steatosis; however, the effect on fibrosis is controversial.

Methods: The effects of pitavastatin (one of the strongest statins) were examined using a choline-deficient L-amino acid-defined (CDAA) diet liver fibrosis model.

Results: Pitavastatin significantly attenuated increases in serum aspartate aminotransferase, alanine aminotransferase, hepatic steatosis, oxidative stress, pre-neoplastic lesions (glutathione S-transferase placental form-positive lesions), expression of cytokines, such as tumor necrosis factor-α and transforming growth factor-β1, and the expression of tissue inhibitor of metalloproteinase-1, tissue inhibitor of metalloproteinase-2 and type I procollagen genes followed by attenuating fibrosis of the liver of CDAA-fed rats.

Conclusion: These results indicate that pitavastatin may inhibit steatosis, hepatic fibrosis and carcinogenesis in rat model of NASH.

Key words: NASH, statin, steatosis, fibrosis

INTRODUCTION

NON-ALCOHOLIC STEATOHEPATITIS (NASH) is a common liver disease that may progress to cirrhosis, liver failure and liver cancer. The histological findings of NASH are characterized by steatosis, hepatic inflammation and injury to liver cells. In patients with highly progressive fibrosis in NASH, the 5-year cumulative incidence of hepatocellular carcinoma (HCC) was 20%[1] and HCC seemed to occur in advanced fibrotic stages in the liver, but the natural history of NASH has not yet been revealed.

Various factors are involved in the transition from non-alcoholic fatty liver disease (NAFLD) to NASH. The two-hit theory postulating the existence of an additional factor (second hit) after steatosis (first hit) has been generally proposed,[2,3] and oxidative stress and insulin resistance in its background are considered to be important. Because the causes of NASH are diverse, no definite therapy has been established. Recently, several reports have revealed the improvement of NASH, such as by the antioxidant vitamin E (α-tocopherol),[4] angiotensin II type 1 receptor blocker (ARB),[5,6] insulin resistance-improving agents[7] and peroxisome proliferator-activated receptor (PPAR)-γ ligand in NASH patients[8] and NASH model rats.[9] On the other hand, some controversial papers have been reported.[10]

Statins, 3-hydroxy-3-methyglutaryl-coenzyme A (HMG-CoA) reductase inhibitors, are well known to reduce low-density lipoprotein (LDL) cholesterol concentrations and to reduce the incidence of coronary heart disease and other major vascular events.[11] Some experimental reports have revealed that statins can reduce liver triglyceride[12] and ameliorate severe hepatic steatosis,[13] and are therefore capable of improving NASH. On the other hand, clinically, the study of statin treatment for NASH is not adequate.[14–16] It has been

Correspondence: Dr Shunsuke Nojiri, Department of Gastroenterology and Metabolism, Nagoya City University Graduate School of Medical Sciences, 1 Kawasumi, Mizuho-cho, Mizuho-ku, Nagoya, Aichi 467-8601, Japan. Email: snojiri@med.nagoya-cu.ac.jp
Received 9 April 2010; revised 27 November 2010; accepted 18 December 2010.

reported that statins improved liver steatosis or the non-alcoholic fatty liver disease activity score but their efficacy for fibrosis is controversial. It is well known that statins have many non-cholesterol-dependent effects as well as cholesterol-lowering effects[17] and some antifibrotic effects have been reported.[18] We therefore hypothesized that statins had inhibiting effects not only on triacylglycerol (TG) consumption and inflammation but also on fibrogenesis and carcinogenesis of the liver. A study of the effects on statins on all these effects in NASH has not been reported. The aim of this study was to investigate the experimental inhibiting effects on steatosis, fibrosis and carcinogenesis of statins in NASH using a rat model and to reveal the clinically useful potential of statins for NASH.

METHODS

Animals

SIX-WEEK-OLD male Wistar rats were purchased from CLEA Japan Inc. (Tokyo, Japan), housed under controlled lighting (12:12-h light : dark cycle), and food and water were freely accessible throughout the study period. Pitavastatin was purchased from Kowa Pharmaceutical (Tokyo, Japan). The choline-deficient L-amino acid-defined (CDAA) diet and choline-supplemented L-amino acid-defined (CSAA) diet were obtained in powder form (Dyets, Bethlehem, PA, USA), as described in previous reports.[19,20] Pitavastatin powder was mixed uniformly into the CDAA and CSAA diets at concentrations of 0 and 5 (mg/kg per day). Based on the national regulations and guidelines, all experimental procedures were reviewed by the Institutional Laboratory Animal Care and Use Committee (IACUC) of Nagoya City University, and were finally approved by the President of the University (no. H19-04).

Experimental protocol

The study periods were 2 and 10 weeks. In the 2-week experiment, two groups of eight rats each received a CSAA diet containing 0 and 5 mg/kg per day pitavastatin, and two groups of eight rats each received a CDAA diet containing 0 and 5 mg/kg per day pitavastatin. In the 10-week experiment, similarly, two groups of eight rats each received a CSAA diet or a CDAA diet containing 0 and 5 mg/kg per day pitavastatin. We measured the amount of food that the rats ate every day to determine the amount of pitavastatin necessary to establish a daily dose of 5 mg/kg of rat weight. As food consumption among the rats was essentially equally, we considered that 5 mg/kg per day pitavastatin was consumed during the experimental periods.

Biochemical parameters

In all experiments, serum aspartate aminotransferase (AST), alanine aminotransferase (ALT) and TG were measured.

Histopathological and immunohistochemical examinations

Five-micrometer-thick sections of the right lobe of all rat livers, fixed in 10% formalin for 24 h and embedded in paraffin, were processed for hematoxylin–eosin and Masson trichrome staining. Glutathione S-transferase placental form (GST-P)-positive lesions (as suitable markers for pre-neoplastic lesions in rat hepatocarcinogenesis)[21] and nitrotyrosine-positive lesions (as oxidant stress)[22] (#06–286 upstate) were immunohistochemically assessed employing the avidin–biotin–peroxidase complex method. Fat drops, fibrosis, nitrotyrosine and GST-P-positive areas in the liver were quantified using a Provis microscope (Olympus, Tokyo, Japan) equipped with a charge-coupled device camera (Sony, Tokyo, Japan), and subjected to computer-assisted analysis with IPAP-WIN software (Sumitomo Techino Service, Hyogo, Japan). Ten different randomly selected areas per specimen were analyzed. The areas of fat drops, fibrosis and nitrotyrosine-positive cells were expressed as a percentage of the total area of the specimen. GST-P-positive lesions were expressed as a percentage of the total area, and the number of GST-P-positive lesions was counted in 10 specimens.

Real-time polymerase chain reaction (PCR) for quantitative assessment of mRNA expression

Tissue inhibitor of metalloproteinase-1 (TIMP-1), tissue inhibitor of metalloproteinase-2 (TIMP-2), matrix metalloproteinase-2 (MMP-2) and tumor necrosis factor-α (TNF-α) have been implicated in fibrosis in NASH, and transforming growth factor-β1 (TGF-β1) is also a key cytokine causing fibrinogenesis in NASH. We therefore examined their expressions.

Total RNA was extracted using Trizol reagent according to the manufacturer's recommended protocol (Life Technologies, Grand Island, NY, USA). RNA extracts were reverse-transcribed with random hexamers and avian myeloblastosis virus reverse transcriptase using a commercial kit (Takara, Kyoto, Japan). Expressions of TIMP-1, TIMP-2, MMP-2, TNF-α, and type I procollagen were evaluated by real-time PCR using an ABI

prism 7000 Sequence Detection system (Applied Biosystems, Tokyo, Japan) according to the manufacturer's protocol. Probes and primers for TIMP-1 (ID: Rn00587558_m1), TIMP-2 (ID: Rn00573232_m1), MMP-2 (ID: Rn02532334_s1), TNF-α (ID: Rn99999017_m1), type I procollagen α1 (ID: Rn00901649_g1) and TGF-β1 (ID: Rn00572010_A1) were purchased from Applied Biosystems. The relative target was glyceraldehyde-2-phosphate dehydrogenase (GAPDH; ID: 4352338E) mRNA in an identical cDNA sample using the standard curve method recommended by the manufacturer.

Western blot analysis

For the analysis of protein expression, liver specimens were disrupted in lysis buffer containing (final concentrations) 25 mmol/L HEPES (pH 7.4), 120 mmol/L NaCl, 5 mmol/L ethylene glycol tetraacetic acid, 10% glycerol, 1% Triton X-100, 50 mmol/L NaF, 100 μM Na-o-vanadate, 5 mmol/L Na-pyrophosphate and protease inhibitor cocktail. After 10 min on ice, lysates were centrifuged on ice for 5 min and either used immediately or stored at −70°C until use. The lysates were dissolved in Laemmli buffer, and then placed in a bath of boiling water for 5 min. Subsequently, each sample was separated by 10% sodium dodecylsulfate polyacrylamide gel electrophoresis and transferred to polyvinylidene fluoride membranes. After blocking with 1% bovine serum albumin in Tris-buffered saline Tween-20 (TBST) (20 mmol/L Tris [pH 8.0], 150 mmol/L NaCl and 0.01% Triton X-100) for 1 h at room temperature, the samples were probed with anti-TGF-β1 (IC.5559-100; Biovision Inc., San Francisco, CA, USA), anti-α-smooth muscle actin (α-SMA) antibody (Dako Japan, Tokyo, Japan), and anti-PPAR-γ antibody (sc-7196 rabbit polyclonal antibody), followed by goat anti-mouse or antirabbit antibody conjugated with horseradish peroxidase. After extensive washing with TBST, membranes were treated with enhanced chemiluminescence reagent (Amersham Pharmacia Biotech Inc., Schenctady, NY, USA). Bands were quantified densitometrically. Where required, the density of each band was normalized by comparison to the β-actin (using ab6276-100 antibody; ABcam, Cambridge, MA, USA) protein bands measured in the same membrane.

Serum TGF-β1 concentration determined by enzyme-linked immunosorbent assay and quantification of TG in liver

The TGF-β1 concentration in serum was measured using an Immunoassay Kit (KAC1688; BioSource). TG was measured using a Triglyceride Quantification Kit (Bio-Vision) according to the instructions.

Human hepatic stellate cell line LX-2

Human hepatic stellate cell line LX-2, which was kindly donated by Dr Scott L Friedman, was used to analyze pitavastatin efficacy for the inactivation of human hepatic stellate cells (HSC).[23] The LX-2 cell line was cultured in Dulbecco's modified Eagle's medium (DMEM) (Nissui Pharmaceutical, Tokyo, Japan) with 10% fetal bovine serum. Cells were seeded at a density of 5.0×10^5 cell/mL in monolayer culture on uncoated 60-mm plastic dishes. All cultures were incubated at 37°C in a humidified atmosphere of 5% air. Medium with or without pitavastatin was changed and, after 24 h, the culture cells were harvested with lysis buffer.

Isolation and culture of HSC and culture HSC

Rat HSC were isolated as described previously with some modifications.[24] In brief, the liver was perfused *in situ* via the portal vein with Ca^{2+}, Mg^{2+}-free Krebs–Ringer (KR) solution followed by 0.1% pronase E (Merck, Darmastadt, Germany) and then 0.032% collagenase (Wako Pure Chemicals, Osaka, Japan) solution at 37°C. The digested liver was minced, and incubated in KR solution containing 0.08% pronase E, 0.04% collagenase and 20 μg/mL DNase (Boehringer-Mannheim, Mannheim, Germany) for 30 min at 37°C (pH 7.3). The resulting suspension was then passed through a nylon mesh. The filtrate was centrifuged at 450 *g* for 8 min. A fraction enriched with HSC was finally obtained by centrifugation in 8.2% Nycodenz (Nycomed Pharma, Oslo, Norway) solution at 1400 *g* for 20 min at 4°C. HSC in the upper white layer were washed by centrifugation at 450 *g* for 8 min, suspended in DMEM containing 10% fetal calf serum (Commonwealth Serum Laboratories, Melbourne, Australia), and supplemented with 100 U/mL penicillin and 100 mU/mL streptomycin (Gibco Laboratories, Life Technologies, Grand Island, NY, USA). Seeding conditions were the same as for cell line LX-2. After incubation for 4 h, non-adherent cells were removed with a pipette and the culture medium was replaced with medium containing pitavastatin or the same concentration of dimethylsulfoxide as a control. Medium with or without pitavastatin was changed every 24 h and cell culture was continued up to 3 days.

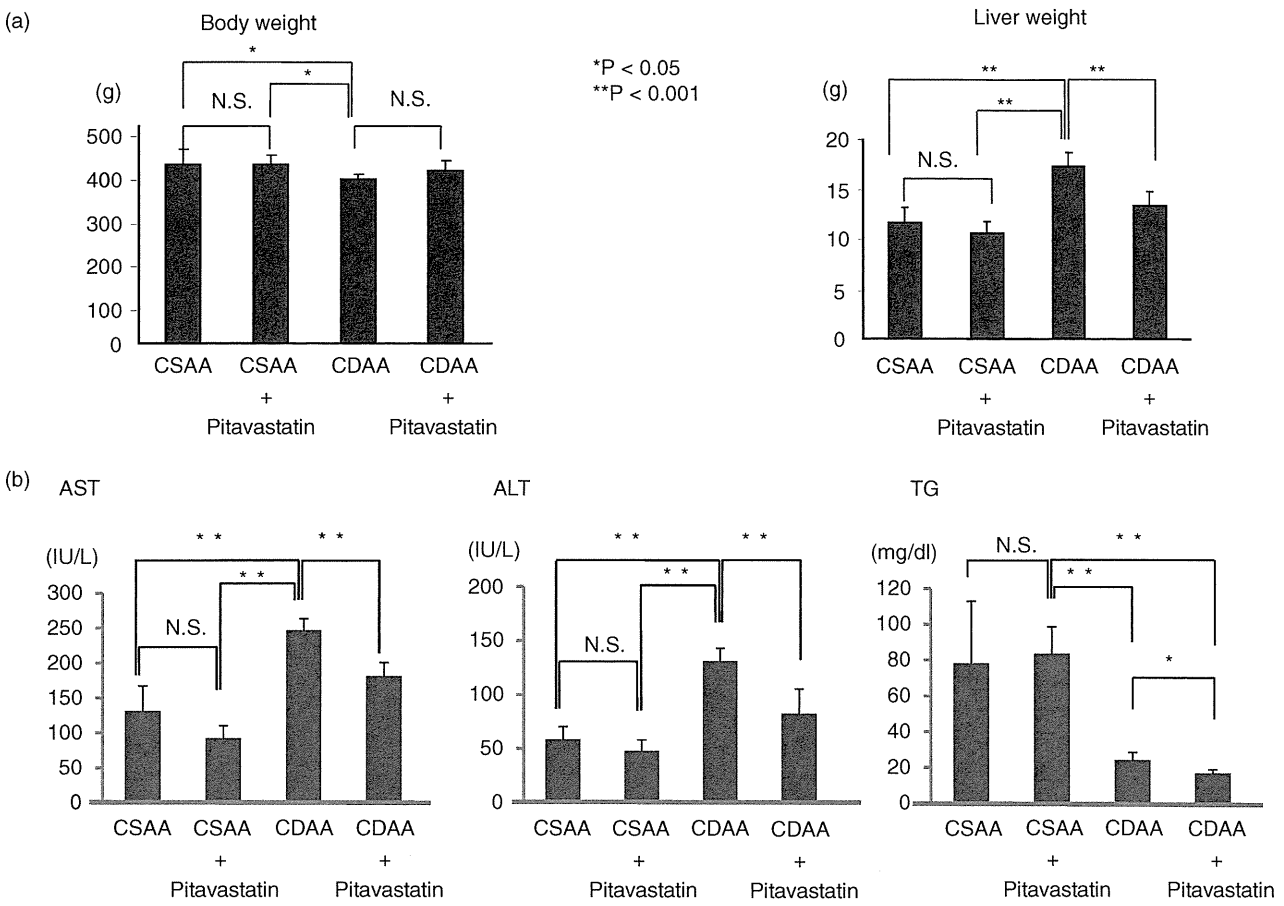

Figure 1 (a) Effect of pitavastatin on the characteristics of rats (10 weeks). Pitavastatin administration did not affect bodyweight changes in choline-supplemented L-amino acid-defined (CSAA)- or choline-deficient L-amino acid-defined (CDAA)-fed rats. The liver weight of CDAA-fed rats significantly increased compared to CSAA-fed rats. The administration of pitavastatin significantly attenuated the liver weight in CDAA-fed rats. (b) Effect of pitavastatin on serum markers (10 weeks). In CDAA-fed rats, aspartate aminotransferase (AST) and alanine aminotransferase (ALT) increased significantly, whereas pitavastatin reduced them. Triacylglycerol (TG) decreased in CDAA-fed rats, and pitavastatin more significantly reduced the level in this model. N.S., not significant.

Statistical methods

Statistical analysis was conducted using ANOVA. The results are expressed as the means ± standard deviation of four or more individual experiments.

RESULTS

Effect of pitavastatin on characteristics of rats

AFTER 10 WEEKS of feeding, the bodyweight of rats fed the CDAA diet was lower than those fed the CSAA diet, and pitavastatin had no influence on bodyweight, whereas rats fed the CDAA diet for 10 weeks showed an increase in the liver weight of 18.5 ± 2.1 g compared with 11.0 ± 0.9 g for rats fed the CSAA diet. Pitavastatin treatment at 5 mg/kg per day in CDAA-fed rats attenuated the increase in liver weight relative to that in CDAA-fed rats that did not receive pitavastatin ($P < 0.001$, Fig. 1a). The serum AST and ALT levels in CDAA-fed rats were significantly higher than in CSAA-fed rats; however, TG was lower in CDAA-fed than in CSAA-fed rats. Treatment of the CDAA-fed rats with pitavastatin decreased both AST and ALT levels (Fig. 1b).

Histological findings of liver steatosis

In this model, after 2 weeks, significant steatosis was observed in CDAA-fed rats, and pitavastatin attenuated

Table 1 Quantitative analysis of liver steatosis in choline-supplemented L-amino acid-defined (CSAA) or choline-deficient L-amino acid-defined (CDAA)-fed rats with or without pitavastatin

Treatment (no. of rats)	After 2 weeks		After 10 weeks	
Fat drop area (mean ± SD) (%)				
CSAA (8)	0	$P < 0.001$	0	$P < 0.001$
CDAA (8)	47.1 ± 5.8		30.7 ± 6.4	
CDAA + pitavastatin (8)	36.8 ± 3.7	$P < 0.001$	20.6 ± 5.0	$P < 0.05$
Quantitative triacylglycerol in the liver of CSAA- or CDAA-fed rats mg/g wet weight (mean ± SD)				
CSAA (8)	2.5 ± 1.9	$P < 0.001$	6.4 ± 2.9	$P < 0.001$
CDAA (8)	557.0 ± 73		201.5 ± 37.8	
CDAA + pitavastatin (8)	420.7 ± 99	$P < 0.001$	144.2 ± 14.6	$P < 0.001$

After 2 and 10 weeks, liver steatosis had progressed in CDAA-fed rats, and pitavastatin (5 mg/kg per day) decreased the development of liver steatosis.
After 2 and 10 weeks, triacylglycerol in the liver tissue had increased significantly in CDAA-fed rats and pitavastatin (5 mg/kg per day) attenuated its accumulation.
SD, standard deviation.

the development of steatosis, and the size of fat drops in hepatocytes of rats fed the CDAA diet with pitavastatin seemed to be smaller than in rats fed the CDAA diet without pitavastatin (data not shown). After 10 weeks, the same tendency was observed but the area of steatosis was reduced due to being occupied by fibrosis, and a lower level of significance was observed between with and without pitavastatin in CDAA-fed rats (Table 1). After 2 and 10 weeks, TG in the liver tissue had increased significantly in CDAA-fed rats and pitavastatin (5 mg/kg per day) attenuated its accumulation (Table 1).

Histological findings of fibrosis

Histological analysis of the livers of CDAA-fed rats at 10 weeks revealed extensive fibrosis and the accumulation of extracellular matrix. In contrast, pitavastatin significantly inhibited the development of liver fibrosis (Fig. 2a) shown with 5 mg/kg per day administration. Image analysis showed that the extent of liver fibrosis in CDAA-fed rats treated with pitavastatin was significantly reduced (Fig. 2ca).

Effect of pitavastatin on oxidative stress and GST-positive lesions in the rat liver (10 weeks)

Nitrotyrosine, a marker of oxidative stress, in liver sections was investigated immunohistochemically. Nitrotyrosine-positive cells were more frequent in the liver sections of CDAA-fed rats, and pitavastatin administration markedly reduced nitrotyrosine-positive cells (Fig. 2b,cb). GST-P-positive lesions consisted mainly of these nodules. It has been reported that GST-P[21] is a suitable marker of pre-neoplastic lesions in rat hepatocarcinogenesis. The results of quantitative analysis were studied. The concomitant administration of 5 mg/kg per day pitavastatin significantly reduced the number and area of GST-P-positive lesions, compared with the livers of rats fed the CDAA diet without pitavastatin (Fig. 3).

Effect of pitavastatin on rat liver fibrogenesis

To investigate the effect of pitavastatin on fibrogenesis and fibrolysis in the rat liver, we assessed mRNA expressions of TIMP-1, TIMP-2, MMP-2 and type I procollagen employing real-time PCR after 10 weeks (Fig. 4). TIMP-1, TIMP-2, MMP-2 and type I procollagen mRNA in the liver significantly increased in CDAA-fed compared to CSAA-fed rats. The addition of 5 mg/kg per day pitavastatin to the CDAA diet significantly reduced the expressions of TIMP-1, TIMP-2, MMP-2 and type I procollagen mRNA in the liver, compared with those of rats fed the CDAA diet without pitavastatin. The addition of 5 mg/kg per day pitavastatin to the CSAA diet caused no changes compared to the CSAA diet without pitavastatin.

Effect of pitavastatin on TNF-α, TGF-β1 and α-SMA

The relative expression of TNF-α mRNA was higher in CDAA-fed than in CSAA-fed rats, and pitavastatin significantly attenuated the expression of TNF-α (Fig. 4).

Protein in the serum and mRNA in the liver of TGF-β1 were examined. The protein levels of TGF-β1